Magnetostrictive Vibration of Prolate Spheroids. Analysis and Experimental Results*

F. J. Beck, J. S. Kouvelites, and L. W. McKeehan
Dunham Laboratory of Electrical Engineering and Sloane Physics Laboratory, Yale University, New Haven, Connecticut†

(Received August 14, 1951)

Small centrally-clamped ferromagnetic specimens are uniformly and axially magnetized by an applied static field. They are simultaneously subjected to an axial *hf* magnetic field and allowed to vibrate longitudinally in the frequency region of their fundamental mode. Through an analysis of this vibrational system, a method is developed whereby from the resonance changes of the impedance of the *hf* magnetizing coil, values may be computed for the incremental permeability, magnetostriction constant, modulus of elasticity, and dissipation constant of the ferromagnetics. Annealed specimens of nickel and of several nickel-iron alloys, as well as the nickel in the unannealed state, were thus tested. The variations of the physical parameters with composition, magnetic bias, and heat treatment, are examined qualitatively in the light of present domain theory and found to be consistent. A good quantitative check of the experimental method is provided by the calculation of the saturation magnetostriction of nickel as -36.7×10^{-6}.

INTRODUCTION

THE magnetostrictive processes are very intimately related to many other physical characteristics of ferromagnetic media. Considerable experimental work[1] has firmly established this fact. Most of the individual experiments, however, have been limited to the quasi-static measurement of a maximum of two physical properties as functions of controlled external conditions. This limitation is not serious as long as the investigators' concern is restricted to reproducible quantities such as the differences in magnetostrictive strain and Young's modulus between the unmagnetized and saturated states. When the variations of the physical parameters for intermediate states of magnetization are of interest, it becomes advisable to measure as many of the parameters as possible simultaneously. Otherwise, any correlation of results of different experiments and any subsequent theoretical deductions are subject to considerable error due to inevitable discrepancies between specimens of similar composition and heat treatment.

We have therefore resorted to measurements of the magnetostrictive vibrational response of ferromagnetic rods. A computational procedure (to be described later), when applied to the results of these measurements, yields accurate values for four physical properties of the specimens, as they concurrently exist for a given set of external conditions.

The performance of our equipment, designed for high frequency measurements of the effects induced in the exciter coil by the vibrational motion of the specimen, is described in a previous paper.[2] Also discussed there are the reasons for the particular size and shape of the specimens (prolate spheroids with major axis 20 mm and minor axes 1 mm).

Some of the basic arguments of our analysis of the magnetostrictively-excited vibrational system pertinent to a prolate spheroid, were first developed by Pierce[3] in his treatment of a magnetostrictively vibrating cylindrical rod. We have leaned more heavily, however, on the later and more refined analysis of the same problem (except for a toroidal specimen) by Butterworth and Smith.[4]

ANALYSIS

The prolate spheroid, bounded by the surface, $b^2x^2+a^2r_1^2=a^2b^2$ (where a, the semimajor axis $\gg b$), was clamped centrally so that it was free to vibrate longitudinally in its fundamental mode. It was placed coaxially in the long, cylindrical exciter coil, of n turns per cm, through which the *hf* current, j, was flowing.

Thoroughly annealed, polycrystalline metals, to which our present experimentation has been mainly restricted, are essentially isotropic elastically as well as magnetically. Hence, since the eccentricity of the spheroid is nearly unity, its equiphase surfaces of displacement, ξ, may be considered to be planes perpendicular to the X-axis. The second law of motion applied to a cross-sectional plane lamina of differential thickness, dx, of the spheroid, may be stated then as

$$(\partial F/\partial x)dx=\pi\rho(b/a)^2(a^2-x^2)(\partial^2\xi/\partial t^2)dx, \qquad (1)$$

where ρ is the mass density. F, the axial force on the lamina, is composed of three parts. The elastic force, F_E, is related to the strain through Hooke's law; thus

$$F_E=\pi E(b/a)^2(a^2-x^2)(\partial\xi/\partial x), \qquad (2)$$

where E is the modulus of elasticity. A dissipative force, F_G, related to the velocity of the strain, is defined in terms of the dissipation constant, G, as

$$F_G=\pi G(b/a)^2(a^2-x^2)(\partial/\partial t)(\partial\xi/\partial x). \qquad (3)$$

Finally, by virtue of Joule's empirical law, there is a magnetostrictive force,

$$F_M=-\lambda\Phi_x, \qquad (4)$$

* This paper is based on a dissertation submitted by J. S. Kouvelites in partial fulfillment of the requirements for the degree of Doctor of Philosophy at Yale University.

† Assisted by the ONR.

[1] Thoroughly outlined in Chapter 13 of R. M. Bozorth, *Ferromagnetism* (D. Van Nostrand Company, Inc., New York, 1950).

[2] J. S. Kouvelites and L. W. McKeehan, Rev. Sci. Instr. **22**, 108 (1951).

[3] G. W. Pierce, Proc. Am. Acad. Arts Sci. **63**, 1 (1928).

[4] S. Butterworth and F. D. Smith, Proc. Phys. Soc. (London) **43**, 166 (1931).

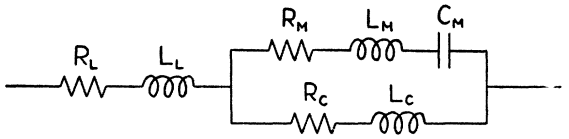

FIG. 1. The equivalent electrical circuit for the magnetostrictive vibrational system.

produced by Φ_x, the axial component of magnetic induction integrated over a cross-sectional area of the spheroid. The negative sign in (4) allows the magnetostriction constant, λ, to be positive when the magnetostrictive effect is positive. Furthermore, Φ_x consists of two parts. One is associated with the exciter coil current. The other, through the inverse magnetostrictive effect: $H=4\pi\lambda(\partial\xi/\partial x)$, is the magnetic flux produced by the mechanical strain. Hence, in terms of the two corresponding magnetic intensities at the surface of the spheroid, the total magnetic flux is

$$\Phi_x=4\pi\mu[n\beta j+\lambda(\partial\xi/\partial x)]W(x), \tag{5}$$

where μ is the magnetic permeability, β is a reducing factor due to the self-demagnetization of the spheroid, and W, an area dimensionally, is a field distribution function.

When Eqs. (2) through (5) are substituted into (1), and it is assumed that ξ and j vary harmonically with time, i.e., $\xi=X(x)e^{i\omega t}$ and $j=Je^{i\omega t}$, the equation of motion takes the form

$$\begin{aligned}[(a^2-x^2)(E+i\omega G)-U](d^2X/dx^2)\\ -[2x(E+i\omega G)+(dU/dx)](dX/dx)\\ +\omega^2\rho(a^2-x^2)X=(n\beta J/\lambda)(dU/dx),\end{aligned} \tag{6}$$

where $U=4\mu W(a\lambda/b)^2$. A solution of this equation, subject to the condition that $X=0$ at $x=0$, would yield X as a linear function of J. Consequently, X could be eliminated from Eq. (5), and the procedure in establishing the relationship between the measured impedances of the exciter coil and the physical constants, would be virtually completed. Unfortunately, even at extremely low frequencies where there are essentially no eddy currents and W becomes $\pi b^2(a^2-x^2)/a^2$, the solutions of (6) are much too unwieldy to allow reasonably fast computation. In fact, for the range of resonant frequencies, permeabilities, and conductivities of the metallic specimens of the present work, the eddy current "skin depth," δ, is much smaller than r_1 over almost the entire specimen length; hence, W takes the form const. $(a^2-x^2)^{\frac{1}{2}}$, making matters even worse.

Although a solution of the equation of motion appears rather impratical, an approximate solution to the vibration problem may be obtained from energy considerations. The normal situation in most crystalline structures vibrating mechanically, is that the potential and kinetic energies far exceed the dissipative losses. It follows that for a spheroidal rod of such a substance, the displacement pattern for forced vibration would be closely that for free vibration in the same mode. It has already been found[5] that for the fundamental mode of free vibration of a prolate spheroid, the displacement varies essentially sinusoidally as a function of x, i.e., $\xi=X_a\sin(\pi x/2a)e^{i\omega t}$. With this displacement configuration, we proceed to sum up the energies of each of the cross-sectional plane lamina to obtain the energies of the entire spheroid. The total kinetic energy is found to be

$$\begin{aligned}T&=\tfrac{1}{2}\int_{x=-a}^{x=a}(\partial\xi/\partial t)^2dm\\ &=-\tfrac{1}{2}\pi(b\omega X_a/a)^2\rho e^{2i\omega t}\int_{-a}^{a}(a^2-x^2)\sin^2(\pi x/2a)dx\\ &=-0.728b^2a\omega^2\rho X_a{}^2e^{2i\omega t}.\end{aligned} \tag{7}$$

With the help of Eq. (2), the elastic-potential energy is determined as

$$V_E=\tfrac{1}{2}\int_{-a}^{a}F_E(\partial\xi/\partial x)dx=3.36(b^2/a)EX_a{}^2e^{2i\omega t}, \tag{8}$$

and the dissipative energy is computed to be

$$V_G=\tfrac{1}{2}\int_{-a}^{a}F_G(\partial\xi/\partial x)dx=3.36i(b^2/a)GX_a{}^2e^{2i\omega t} \tag{9}$$

by means of Eq. (3). To obtain an expression for the magnetostrictive energy, V_M, it is necessary first to determine Φ_x in terms of x. As discussed in the Appendix, the equations resulting from a rigorous analysis of the field configuration problem, are not readily solvable. However, since the field in the specimens of this study diminishes rapidly with penetration, two simplifications can be made with regard to Eq. (5). First, it is easily found that β is very nearly unity (i.e., negligible *hf* self-demagnetization). Secondly, the magnetic field distribution within the spheroid is essentially that of a semi-infinite solid, whose well-known solution integrated over a cross section gives

$$\begin{aligned}W&=\int_0^{2\pi}\int_0^{r_1}\exp[-(1+i)(r_1-r)/\delta]rdrd\theta\\ &=\pi\delta\{(1+i)r_1+i\delta-i\delta\exp[-(1+i)r_1/\delta]\}\\ &\simeq\pi\delta[(1+i)r_1+i\delta]\text{ for }\delta\ll r_1.\end{aligned} \tag{10}$$

With the help of (5) and (10), it is now possible to evaluate V_M as

$$\begin{aligned}V_M&=\tfrac{1}{2}\int_{-a}^{a}F_M(\partial\xi/\partial x)dx\\ &\simeq-\mu\lambda N[36.2nJ+44.2\lambda X_a/a]\end{aligned} \tag{11}$$

where $N=(1-i)\delta b+1.17i\delta^2$.

[5] J. S. Kouvelites, Quart. Appl. Math. **9**, 105 (1951).

To satisfy the conservation of energy principle, the sum of the energies must equal zero. Hence, from (7), (8), (9), and (11), we obtain

$$[3.36(E+i\omega G)-0.728\omega^2a^2\rho]b^2X_a - \mu\lambda N(36.2anJ+44.2\lambda X_a)=0. \quad (12)$$

Moreover, the electromotive force induced in the exciter coil by the *hf* magnetic flux passing through the spheroid, may be stated as

$$e=n\int_{-a}^{a}(\partial\Phi_x/\partial t)dx \simeq i\omega n\mu N(59.2anJ+72.2\lambda X_a)e^{i\omega t}. \quad (13)$$

Combining the last two relationships to eliminate X_a and remembering that $\delta=1/[2\pi(f\sigma\mu)^{\frac{1}{2}}]$ in emu, where σ is the electrical conductivity, we arrive at the expression for an impedance,

$$Z=e/j=Z_cZ_M/(Z_c+Z_M),$$

where

$$Z_c=59.2abn^2[(1+i)(f\mu/\sigma)^{\frac{1}{2}}-0.186/\sigma b] \quad (14)$$

and

$$Z_M=4.50a(bn/\lambda)^2[\omega^2G+i\omega(\omega^2/\omega_0^2-1)E],$$

$\omega_0=(4.62E/a^2\rho)^{\frac{1}{2}}$ being the resonant angular frequency for free vibration in the fundamental mode.[5] From Eqs. (14), it appears that Z, the impedance of the exciter coil produced by the total magnetic flux of the spheroid, may be represented as the impedance of an electrical circuit consisting of a parallel combination of Z_c and Z_M. Both Z_c, the "clamped" impedance, and Z_M, the "motional" impedance, may be broken down to the series combinations of resistive, inductive, and capacitive elements, $Z_c=R_c+i\omega L_c$ and $Z_M=R_M+i(\omega L_M+1/\omega C_M)$. Because of magnetic hysteresis, the incremental permeability is a complex quantity and may be written as $\mu_\Delta e^{-i\eta}$. The components of Z_c and Z_M are then found from Eqs. (14) to be

$$\left.\begin{aligned} R_c&=59.2abn^2[(\cos\tfrac{1}{2}\eta+\sin\tfrac{1}{2}\eta)(f\mu_\Delta/\sigma)^{\frac{1}{2}}-0.186/b\sigma],\\ L_c&=9.43abn^2(\cos\tfrac{1}{2}\eta-\sin\tfrac{1}{2}\eta)(\mu_\Delta/f\sigma)^{\frac{1}{2}},\\ R_M&=4.50(\omega bn/\lambda)^2aG,\\ L_M&=4.50(\omega bn/\omega_0\lambda)^2aE\\ &\simeq 4.50(bn/\lambda)^2aE \text{ near resonance, and}\\ C_M&=1/\omega_0^2L_M. \end{aligned}\right\} \quad (15)$$

Finally, a series combination of the resistance, R_L, and the inductance, L_L, is added to the circuit to account for the electrical resistance of the coil and for the magnetic flux "leakage." The equivalent electrical circuit for the vibrational system is then complete as shown in Fig. 1.

The resonance characteristics of this circuit have been fully investigated.[4] It will suffice here to restate some of its more pertinent properties. By means of the definitions,

$$Z_c=|Z_c|e^{i\phi_c} \quad \text{and} \quad Z_c+Z_M=(R_c+R_M)e^{i\phi_{Mc}}/\cos\phi_{Mc},$$

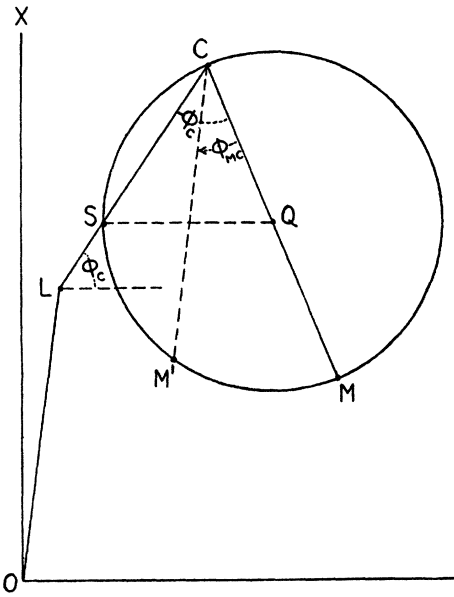

FIG. 2. Complex impedance plane, $OL=Z_L$, $LC=Z_c$, and $CM=Z_c^2/(R_c+R_M)$. Points C and S are referred to in Table I.

TABLE I. The procedure for the determination of the physical parameters from the experimental state.

Quantity	Method of determination
σ; ρ	Resistance, volume, and mass measurements of 15-cm-long wire of the same material (in the same state) as the specimen
Impedance-circle points and corresponding frequencies	Impedance-bridge measurements (with specimen)
R_L	Impedance-bridge measurements (without specimen)
Point C; S; f_1; ϕ_c	Trial-and-error selection until $\tan\phi_{Mc}/(f-f_1)$ is a constant
R_c	$R_c=(R_x$ at pt. $C)-R_L$
L_c	$L_c=159R_c\tan\phi_c/f_1$
R_M	$R_M=\dfrac{[(R_x \text{ at pt. } S)-R_L]R_c}{(R_x \text{ at pt. } C)-(R_x \text{ at pt. } S)}$
L_M	$L_M=79.7(R_M+R_c)\left(\dfrac{\tan\phi_{Mc}}{f-f_1}\right)-L_c$
η	$\tan\dfrac{\eta}{2}=\dfrac{1+N-\tan\phi_c}{1+N+\tan\phi_c}$, $N=11.0an^2/R_c\sigma$
μ_Δ	$\mu_\Delta=\dfrac{f_1\sigma}{89.0(1-\sin\eta)}\left(\dfrac{L_c}{abn^2}\right)^2$
E	$E=8.57(10)^6(1+L_c/L_M)f_1^2a^2\rho$
$\pm\lambda$	$\pm\lambda=0.067[aE/L_M]^{\frac{1}{2}}bn$
G	$G=0.217(10)^6a^2\rho(R_M/L_M)(1+L_c/L_M)$

Units:

ρ	gm/cm³	n	turns/cm
σ	mho/cm	μ_Δ	gauss/oersted
R	ohm	E	dyne/cm²
L	μh	λ	dyne/cm² gauss
f	kc/sec	G	dyne sec/cm²
a, b	cm		

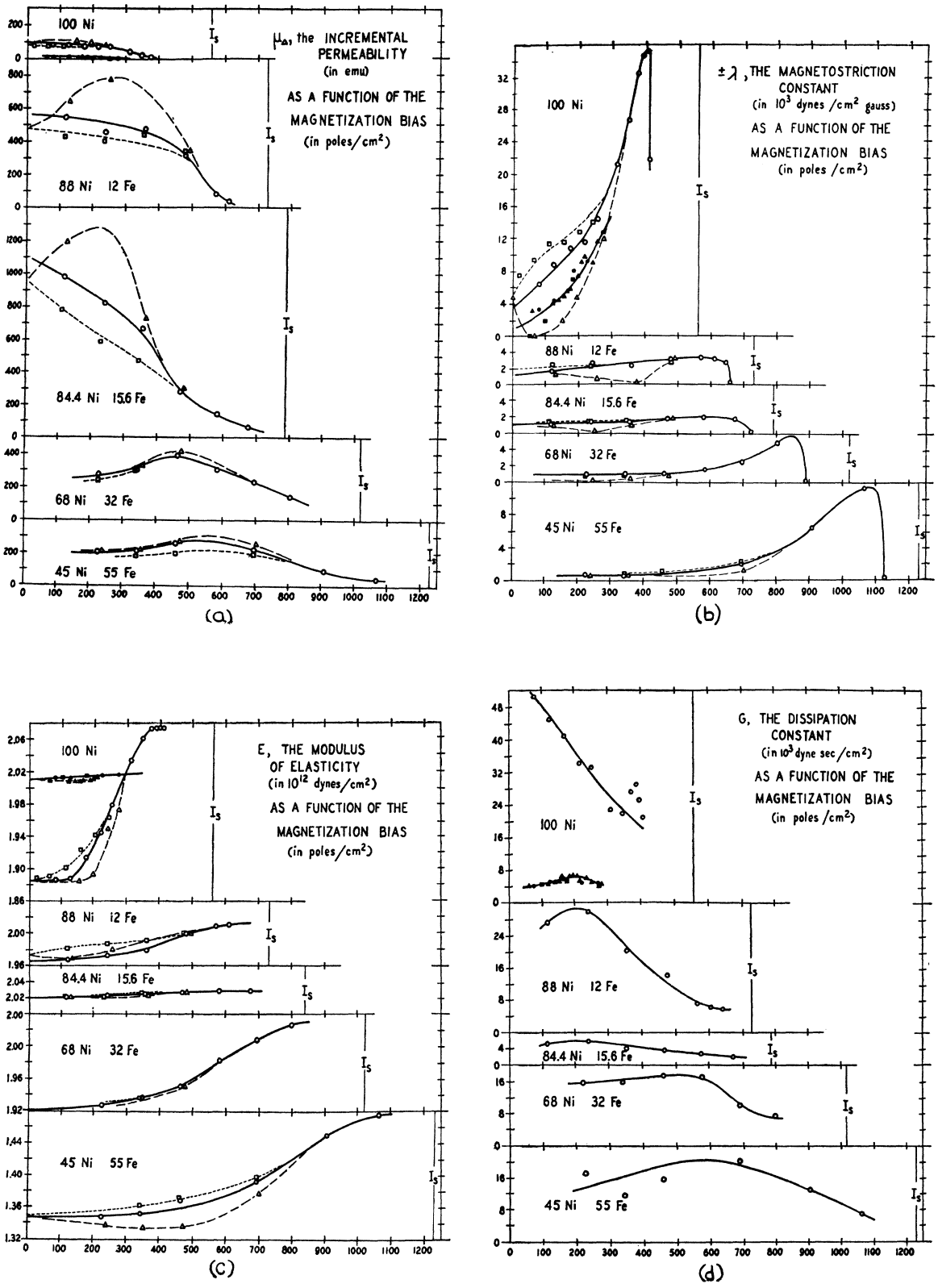

FIG. 3. Experimental results. The experimental points for the unannealed nickel are solidly black. The solid curves correspond to the static magnetization curves. The long dashes represent a bias decreasing from saturation on a hysteresis loop, while a hysteresis-loop-bias increasing to saturation is represented by the short dashes.

the total impedance of the circuit may be expressed as

$$Z_X = Z_L + Z_c Z_M/(Z_c+Z_M)$$
$$= Z_L + Z_c - |Z_c|^2 \cos\phi_{Mc} e^{i(2\phi_c - \phi_{Mc})}/(R_c+R_M), \quad (16)$$

the last term describing a circular variation of Z_X on the impedance plane for changes of ϕ_{Mc}. Near resonance, ϕ_{Mc} varies sharply with frequency in the manner found to be

$$\tan\phi_{Mc} \simeq 2(\omega-\omega_1)(L_c+L_M)/(R_c+R_M), \quad (17)$$

where $\omega_1^2 = 1/(L_c+L_M)C_M$. The variation of Z_X with frequency is shown on the impedance plane of Fig. 2 as the circular locus of M'.

From the resonance properties of the equivalent electrical circuit and from Eqs. (15), a systematic method was developed for facile calculation of the defined physical constants. This method is outlined in Table I, where the experimental and computational steps must be taken in the indicated sequence. The points referred to in this table are the points appropriately labeled in Fig. 2. Some of the quantities have been converted from emu to practical units in which they are more commonly measured.

EXPERIMENTAL RESULTS

To substantiate the correctness of our analysis of the vibrational system and the utility of the resulting computational scheme, we chose to study by the method outlined, the properties of the γ-phase Ni-Fe alloy series, the permalloys, at room temperature. It has long been established that the magnetostriction of the permalloy of approximately 81 percent nickel is zero, while for compositions with less or more nickel the magnetostriction is, respectively, positive or negative.[6] Since there are theoretical reasons to believe that other physical properties also will behave singularly at this critical composition,[7,8] the polycrystalline materials selected for this study consisted of one close to this composition, two with less nickel, and two with more nickel (including the commercially pure nickel specimen). After being ground to shape, the spheroidal specimens were all annealed for three hours at 650°C in a hydrogen atmosphere and then furnace-cooled. The nickel specimen, however, was investigated before this heat-treatment as well as after.

The hf impedance measurements were made of the magnetostrictive vibrational response of each specimen while it was biased either on its static magnetization curve (as usual, achieved by many reversals of magnetization) or on a large hysteresis loop. The amplitude of the exciting field was kept constant at 1.4 oersted. The values of μ_Δ, $\pm\lambda$, E, and G computed from this data are shown in Fig. 3 (a) to (d), respectively, as functions of the magnetization bias. The estimated value for the saturation magnetization, I_s, of each material is indicated as a reference level. It should be noted that only the absolute magnitude of λ may be obtained by means of Table I. Some previous knowledge of the "sign" of the magnetostriction of the test-material is therefore always required. In Fig. 3(b), λ is positive for the 45 and 68 percent—nickel permalloys, and negative for the other three compositions.

The errors in the evaluation of the physical parameters from impedance circle-diagrams arise in the determination of the size of the circles, of the rate of frequency variation about their circumferences, and of the location of the clamped impedance point (point C in Fig. 2). They are estimated to be 0.1 percent for E, 5 percent for μ_Δ, λ, and G, and at least 10 percent for η. The calculated values of η are therefore much too inaccurate to be plotted for even qualitative study.

The magnetostriction constant, λ, as defined by Eq. (4), is equal to the slope of the static magnetostrictive stress-*versus*-magnetic flux density curve, if time lag effects are negligible. Consequently, when λ is multiplied by 4π and divided by the value of the modulus of elasticity for the corresponding bias, the area under the curve of this quantity plotted against the magnetization bias, is essentially equal to the magnetostrictive strain. From the values of λ and E for the annealed nickel [Figs. 3(b) and 3(c)] passed through this integration process, the saturation magnetostriction was calculated to be -36.7×10^{-6} which agrees quite well with previous quasistatic measurements.[9]

A qualitative comparison of the different annealed specimens based on their static magnetization curves, reveals in several ways the expected uniqueness of a composition near 81 percent nickel. From Figs. 3(a) to 3(d), it is observed that the closer the composition was to this critical value, the larger was the maximum incremental permeability, and the smaller were the saturation magnetostriction, the saturation change of Young's modulus, and the maximum dissipation factor. The dissipation factor, incidentally, is associated only with magnetomechanical hysteresis and micro eddy current losses since the losses due to *macro* eddy currents have been accounted for in the hf field distribution equations.

It is interesting enough that as the bias was taken around a hysteresis loop, μ_Δ, λ, and E for each annealed material had different magnitudes of the two hysteresis loop branches for the same magnetization. This was especially evident at small biases. However, it is perhaps more significant that the variations of these parameters about the hysteresis loop appear to be interrelated. For example, as the magnetization was decreased from saturation, the incremental permeability increased rapidly to a maximum at a magnetiza-

[6] L. W. McKeehan and P. P. Cioffi, Phys. Rev. **28**, 146 (1926).
[7] M. Kersten, Z. Physik **76**, 505 (1932); and **85**, 708 (1933).
[8] R. Becker and W. Döring, *Ferromagnetisimus* (Springer, Berlin, 1939), pp. 157–167, 339–348, 365–371.
[9] See reference 8, p. 279.

tion other than zero. At this particular bias, the magnetostriction constant dropped essentially to zero. Since λ is associated with rotations of ferromagnetic domains and μ_Δ with domain reversals, it may be deduced that in this portion of the hysteresis loop, the domains were only reversing discontinuously in response to the hf field. In this bias region, the small variation of the elasticity modulus, known not to be affected significantly by domain reversals, adds support to this conclusion.

The mode of variation of the dissipation constant with bias, for the specimens biased on their static magnetization curves, was similar to that of the incremental permeability. Hence, it is strongly suggested that the losses are a direct manifestiation of irreversible domain boundary displacement. Because of the inherent inaccuracies of the measurements, it was difficult to establish any trends in the variation of the dissipation constant with hysteresis-loop-bias.

The large internal strains of the unannealed nickel undoubtedly hampered the growth and mobility of the magnetic domains. Hence, in harmony with current theory,[7] the maximum μ_Δ, maximum G, and ΔE effect were considerably lower than for its annealed state.

The quantitative agreement of the calculated saturation magnetostriction values and the qualitative correspondence of most of our other experimental results, with previous theory and experimentation, give ample support to our analysis and use of magnetostrictive vibration. Incorporating some small improvements such as the use of a smaller hf field, we are presently exploting some of the promising possibilities of this method in the determination of precise relationships between various physical properties of ferromagnetics.

APPENDIX: FIELD DSITRIBUTION PROBLEM

The Maxwellian field equations applicable within the longitudinally-vibrating prolate spheroidal conductor are

$$\nabla\times\mathbf{H}=4\pi\sigma\mathbf{E}+\epsilon(\partial\mathbf{E}/\partial t)/c^2 \tag{1a}$$

and

$$\nabla\times\mathbf{E}=-\mu(\partial\mathbf{H}/\partial t)+\mu\nabla\times(\mathbf{v}\times\mathbf{H}), \tag{1b}$$

while outside the spheroid, the equations

$$\nabla\times\mathbf{H}=\epsilon(\partial\mathbf{E}/\partial t)/c^2 \tag{2a}$$

and

$$\nabla\times\mathbf{E}=-\mu(\partial\mathbf{H}/\partial t) \tag{2b}$$

apply, the divergences of the electric and magnetic intensity vectors, $\mathbf{E}$ and $\mathbf{H}$, being everywhere zero. Moreover, the term, $\epsilon(\partial\mathbf{E}/\partial t)/c^2$, in (1a) and (2a) is negligibly small since the resonance frequencies for the 2 cm-long Ni and Ni-Fe specimens are all in the order of 150 kc/s; hence, from the above equations, are derived the expressions,

$$\nabla\cdot\nabla\mathbf{H}=4\pi\sigma\mu[(\partial\mathbf{H}/\partial t)-\nabla\times(\mathbf{v}\times\mathbf{H})] \tag{3}$$

and

$$\nabla\cdot\nabla\mathbf{H}=0, \tag{4}$$

which are valid inside and outside the spheroid, respectively. From previous discussion, the displacement, $\xi=\mathbf{X}e^{i\omega t}$, and velocity. $\mathbf{v}=i\omega\mathbf{X}e^{i\omega t}$. Thus, when $\mathbf{H}$ expanded into its Fourier series components:

$$\mathbf{H}_{(0)}+\mathbf{H}_{(1)}e^{i\omega t}+\mathbf{H}_{(2)}e^{2i\omega t}+\cdots,$$

is substituted into (3), and the sum of the coefficients of each of the frequency terms is set equal to zero, it is found that

$$\nabla\cdot\nabla\mathbf{H}_{(n)}=4\pi i\omega\sigma\mu[n\mathbf{H}_{(n)}-\nabla\times(\mathbf{X}\times\mathbf{H}_{(n-1)})], \tag{5}$$

where $n=0, 1, 2, \cdots$. Since only the fundamental component of $\mathbf{H}$ induces an electromotive force in the exciter coil that is not filtered out in the measurements, (5) is consequential only for $n=1$. Furthermore, $\mathbf{H}_{(0)}$, the static bias field, is everywhere axial and uniform within the spheroid, and $\mathbf{X}\times\mathbf{H}_{(0)}=0$. We arrive, therefore, at the expressions,

$$\nabla\cdot\nabla\mathbf{H}_{(1)}=4\pi i\omega\sigma\mu\mathbf{H}_{(1)} \tag{6}$$

and

$$\nabla\cdot\nabla\mathbf{H}_{(1)}=0, \tag{7}$$

which, subject to the boundary conditions, completely define $\mathbf{H}_{(1)}$ inside and outside the conductor.

The boundary conditions are most conveniently expressed by means of prolate spheroidal coordinates, whose orthogonal surfaces are confocal prolate spheroids $[(u^2-1)x^2+u^2r^2=d^2u^2(u^2-1)]$, confocal hyperboloids of two sheets $[(1-v^2)x^2-v^2r^2=d^2v^2(1-v^2)]$, and planes perpendicular to the YZ plane that pass through the X-axis [constant ϕ], $2d$ being the interfocal distance. $\mathbf{H}_{(1)}$ has only u and v components, and they do not vary with ϕ. Therefore, the vector potential, defined by $\nabla\times\mathbf{A}=\mathbf{H}_{(1)}$ and $\nabla\cdot\mathbf{A}=0$, has only a ϕ component, and it also is invariant with ϕ. The equations,

$$\nabla\cdot\nabla\mathbf{A}_i=4\pi i\omega\sigma\mu\mathbf{A}_i \tag{8}$$

and

$$\nabla\cdot\nabla\mathbf{A}_0=0, \tag{9}$$

for the potentials inside and outside the spheroid are derived directly from (6) and (7). Expressed in spheroidal coordinates, (8) is then separated in terms of these coordinates by the assumption of the usual product solution, $A_i=U_i(u)V_i(v)$. Both U_i and V_i are found to be described by the same equation,

$$\frac{d}{du}\left\{(1-u^2)\frac{dU_i}{du}\right\}+\left(\beta_i-\frac{1}{1-u^2}+ku^2\right)U_i=0, \tag{10}$$

where β_i is the separation constant and $k=4\pi i\omega\sigma\mu d^2$. Similarly, by letting $A_0=U_0V_0$, we find that the

equation,

$$\frac{d}{du}\left\{(1-u^2)\frac{dU_0}{du}\right\}+\left(\beta_0-\frac{1}{1-u^2}\right)U_0=0, \quad (11)$$

is appropriate for both U_0 and V_0.

Equation (10) has already been solved by Page and Adams[10] for small, real values of k. Their solution is also valid for a small, imaginary k, but unfortunately, the magnitudes of k for the specimens of this study were in the order of a few thousand. Another method,[11] however, has proved fruitful for the case of large but real values of k, and it offers possibilities which we hope to pursue soon. The fact that k may be complex due to magnetic hysteresis, is not expected to help matters.

The authors wish to thank Mr. R. V. Dyba for his capable assistance in the experimentation.

[10] L. Page and N. I. Adams, *Electrodynamics* (D. Van Nostrand Company, Inc., New York, 1940), Sec. 80.

[11] Stratton, Morse, Chu, and Hutner, *Elliptic Cylinder and Spheroidal Wave Functions* (John Wiley and Sons, Inc., New York, 1941).

PHYSICAL REVIEW VOLUME 84, NUMBER 5 DECEMBER 1, 1951

The Alpha-Particle Disintegration of Beryllium*

WILLIAM O. MCMINN, M. B. SAMPSON, AND V. K. RASMUSSEN
Physics Department, Indiana University, Bloomington, Indiana

(Received August 27, 1951)

The disintegration of Be^9 by 21.7-Mev alpha-particles has been studied with observations of the emitted particles made at various angles. Q-values of -6.92, -7.87, -8.57, and -10.74 Mev were found for the $Be^9(\alpha, p)B^{12}$ reaction giving levels in B^{12} at 0.95, 1.65, and 3.82 Mev. Two groups of deuterons from $Be^9(\alpha, d)B^{11}$ were found giving a level in B^{11} at 2.18 Mev. A third group, if assigned to this reaction would give a level in B^{11} at 0.65 Mev. The inelastic scattering $Be^9(\alpha, \alpha')Be^{9*}$ gives a level in Be^9 at 2.63 Mev.

I. INTRODUCTION

THE charged particle groups produced in the bombardment of thin beryllium films with 21.7-Mev alpha-particles have been investigated by determining their ranges in aluminum absorbers. A preliminary report has been made of some of the results of this investigation which were obtained with apparatus where the angle between the beam direction and the axis of the detecting system was 90°.[1] This report presents the results from observations of the particles emitted in various directions with respect to the direction of the incident particles. This permits the more certain assignment of a group to a definite reaction. The occurrence of the $Be^9(\alpha, d)B^{11}$ reaction is revealed, which was not suspected in our earlier work.

The results of proton scattering experiments by several investigators indicate the lowest excited state of Be^9 to be about 2.42 Mev.[2] Van Patter *et al.* assign two groups obtained by magnetic analysis of the products of the deuteron bombardment of boron to the $B^{11}(d, \alpha)Be^9$ reaction.[3] The Q-values obtained indicate an excited state of Be^9 at 2.422 ± 0.005 Mev.

No excited state below 2.1 Mev has been reported for B^{11}. This level has been obtained from the $B^{10}(d, p)B^{11}$ reaction as 2.138 ± 0.014 Mev by Van Patter *et al.*[4] Li and Whaling[5] have reported a tentative value of 2.107 ± 0.017 Mev from the $C^{13}(d, \alpha)B^{11}$ reaction.

Hudspeth and Swann[6] found a level in B^{12} at about 1 Mev from the deuteron bombardment of boron. Buechner *et al.*,[7] using the same reaction, got a value of 0.947 ± 0.005 Mev. Bockelman[8] found a resonance in the neutron cross section of boron for neutrons of 0.43 Mev which he attributed to the formation of B^{12}. This energy gives a level in B^{12} at 3.70 Mev.

II. EXPERIMENTAL METHOD

The charged particles produced in the alpha-particle bombardment of beryllium were detected with a proportional counter biased to count particles only near the end of their paths. Corrections were made for variations in the beam intensity by monitoring the current which was collected after passing through the thin target foil. A current integrator circuit was used for this purpose.[9]

The beam energy was determined by measuring the ranges of the alpha-particle groups elastically scattered

* Supported by the joint program of the ONR and AEC.

[1] McMinn, Sampson, and Bullock, Phys. Rev. **78**, 296 (1950).

[2] K. E. Davis and E. M. Hafner, Phys. Rev. **73**, 1473 (1948); E. H. Rhoderick, Proc. Roy. Soc. (London) **201**, 348 (1950); Browne, Williamson, Craig, and Donahue, Phys. Rev. **83**, 179 (1951).

[3] Van Patter, Sperduto, Huang, Strait, and Buechner, Phys. Rev. **81**, 233 (1951).

[4] Van Patter, Buechner, and Sperduto, Phys. Rev. **82**, 248 (1951).

[5] C. W. Li and W. Whaling, Phys. Rev. **82**, 122 (1951).

[6] E. L. Hudspeth and C. P. Swann, Phys. Rev. **76**, 1150 (1949).

[7] Buechner, Van Patter, Straight, and Sperduto, Phys. Rev. **79**, 262 (1950).

[8] C. K. Bockelman, Phys. Rev. **80**, 1011 (1950).

[9] H. T. Gittings, Rev. Sci. Instr. **20**, 325 (1949).